Structure determination of liquid biofuels *via in situ* cryocrystallisation and single crystal X-ray diffraction

Siriyara Jagannatha Prathapa, Cara Slabbert,[a,b] Manuel A. Fernandes and Andreas Lemmerer*[a]

a. Molecular Sciences Institute, School of Chemistry, University of the Witwatersrand, Johannesburg 2050, South Africa. Fax: +27 11 717 6749; Tel: +27 11 717 6711; E-mail: Andreas.Lemmerer@wits.ac.za; cara.slabbert@up.ac.za

b. Department of Chemistry, University of Pretoria, Pretoria, 0002, South Africa.

Supplementary Information

Table of Contents

A. *In-Situ* Cryocrystallization via OHCD technique:

Single crystals of the liquid FAMEs were grown *via in-situ* crystallization in a 0.3 mm diameter Lindemann (X-ray transparent glass) capillary using an Optical Heating and Crystallization Device (OHCD III). In this technique samples are loaded into a capillary, sealed on both sides is mounted vertically in the diffractometer (D8 VENTURE) then cooled down to crystallization temperature (just below the melting temperature) using a cold stream of liquid nitrogen. Diffraction quality crystals are created using a zone-melting technique where a small region of the capillary is heated with a CO_2 IR laser to create a molten zone. The laser intensity was increased from zero in 3 minutes to create the molten zone which is sample dependent (Table S1). Then the molten zone is slowly moved along the length of the capillary at about 3cm/30min by adjusting the position of the laser, allowing recrystallization of the molten zone.[1,2] After each cycle intensity was reduced back to zero in 3 minutes. This cycle is repeated several times until a single crystal amenable for diffraction is obtained. Crystals successfully grown this way are then analysed at the atomic level by X-ray diffraction. The number of cycles, cycle time and laser intensity required to obtain a good quality single crystal is sample dependant, and the whole process, which is labour intensive, can take several days. (For a few compounds several attempts have been required resulting in weeks of work). Since the samples are sensitive to temperature and melt easily, the whole experiment is carried out in the measurement device (a diffractometer) hence the term *in situ*.

Table S1. Values of Zone-Melting temperature and the corresponding laser intensity used in the method of *In-Situ* Cryocrystallization of FAMEs.

FAMEs	Zone-Melting Temperature (°)	Laser Intensity
C_5	-114	21
C_6	-77	19
C_7	-70	20
C_8	-46	18
C_9	-44.5	19
C_{10}	-23	21
C_{11}	-25	20
C_{12}	-5	24
C_{13}	-8	22

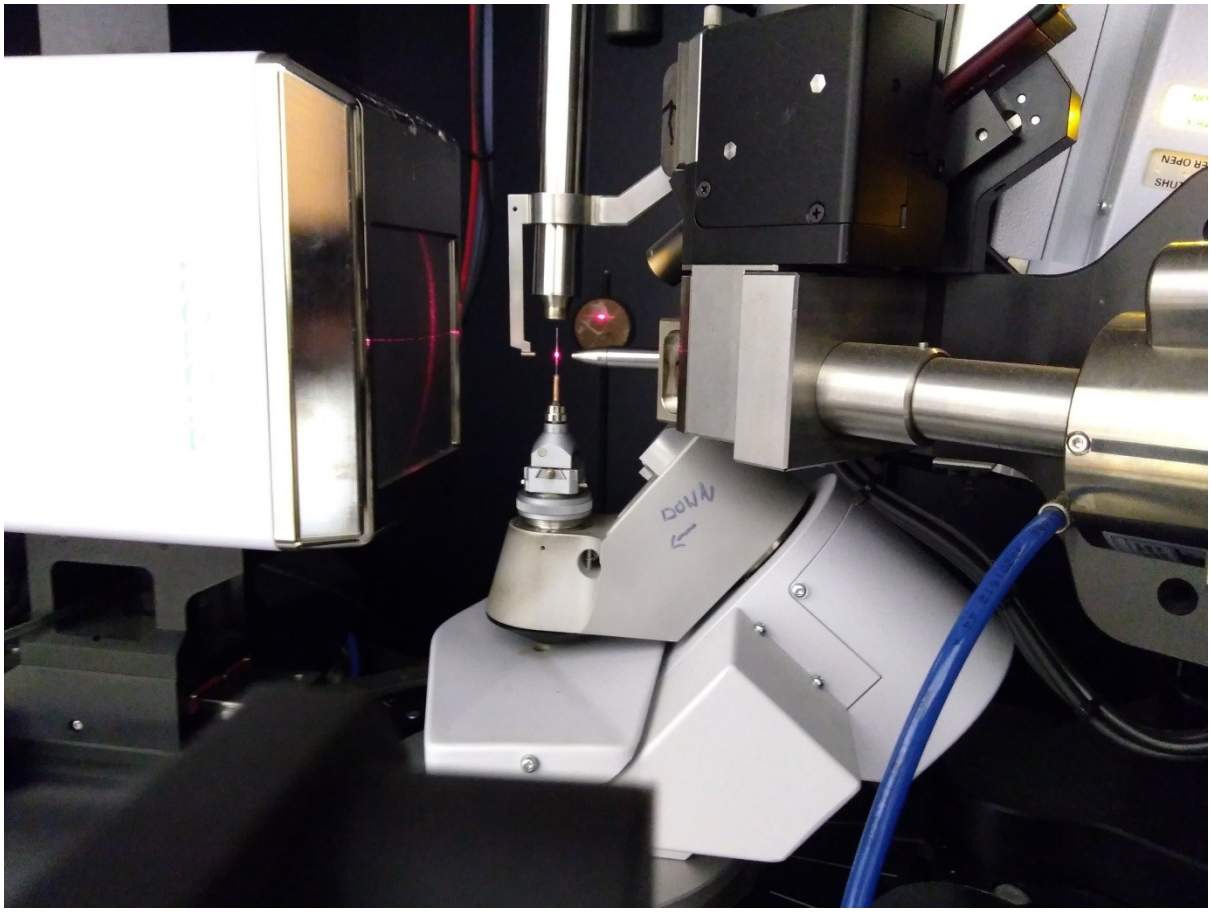

Figure S1. Experimental set up of In-Situ Cryocrystallization via OHCD technique on BRUKER D8 VENTURE X-ray diffractometer.

B. *ORTEP* and Packing Diagrams of FAMEs

B.1 *ORTEP* and Packing Diagrams for C_5 Methyl Ester:

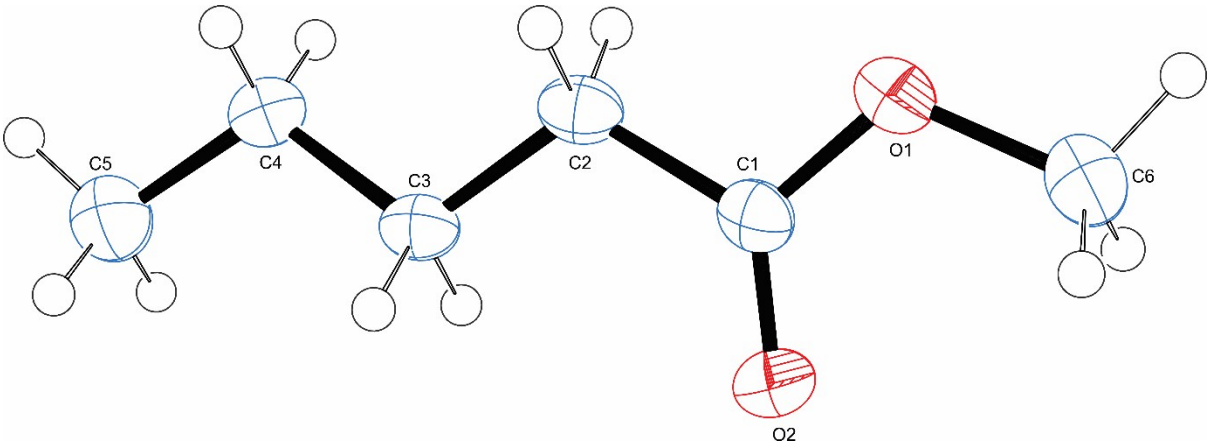

Figure S2. The *ORTEP* diagram of C_5 methyl ester with displacement ellipsoids drawn at the 50% probability level and H atoms are shown as small spheres of arbritary radii.

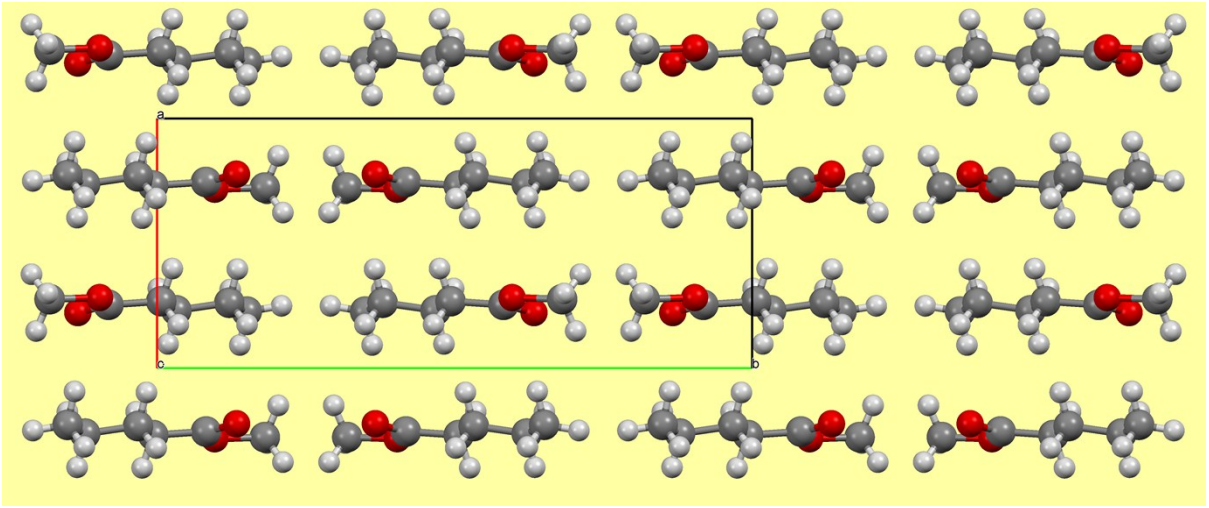

Figure S3. Packing diagram of C_5 methyl ester down the *c*-axis, showing the head-to-head arangement.

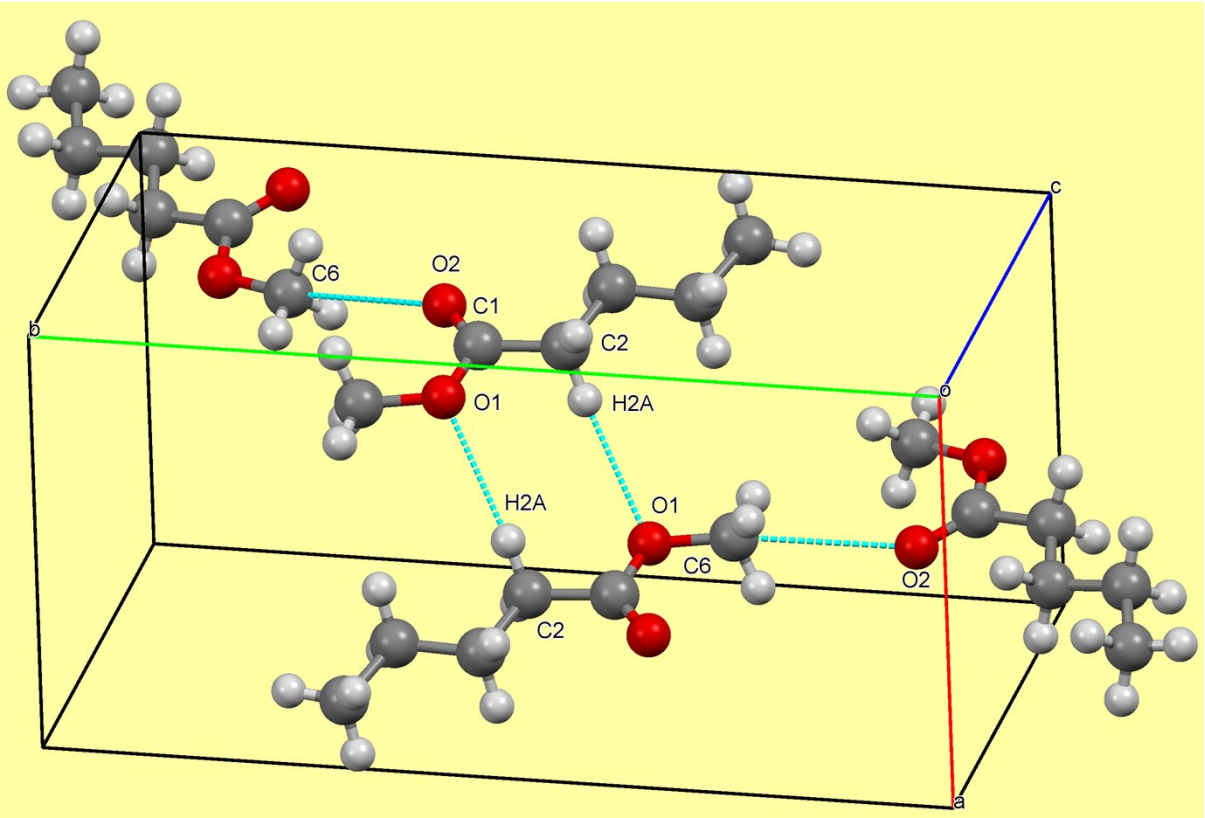

Figure S4. Hydrogen bonding and short contact packing diagram of C_5 methyl ester, , showing the C2-H2A···O1 hydrogen bond and C6···O2 short contact.

B.2 *ORTEP* and Packing Diagrams for C_6 Methyl Ester:

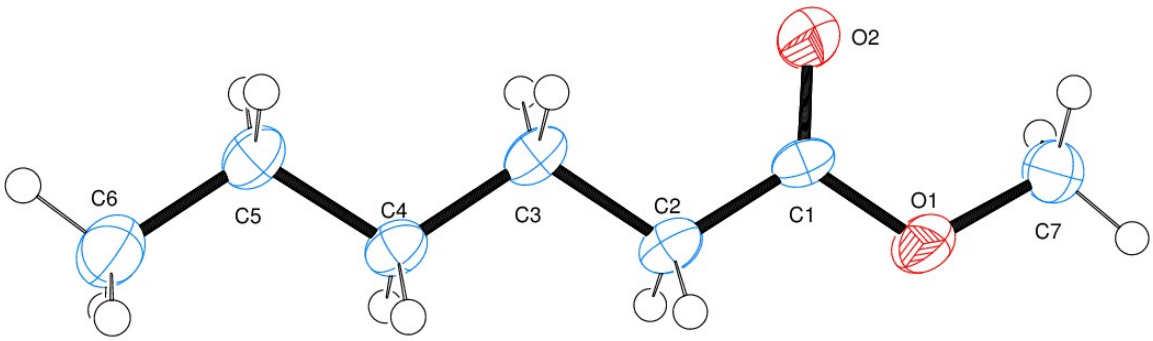

Figure S5. The *ORTEP* diagram of C_6 methyl ester with displacement ellipsoids drawn at the 50% probability level and H atoms are shown as small spheres of arbritary radii.

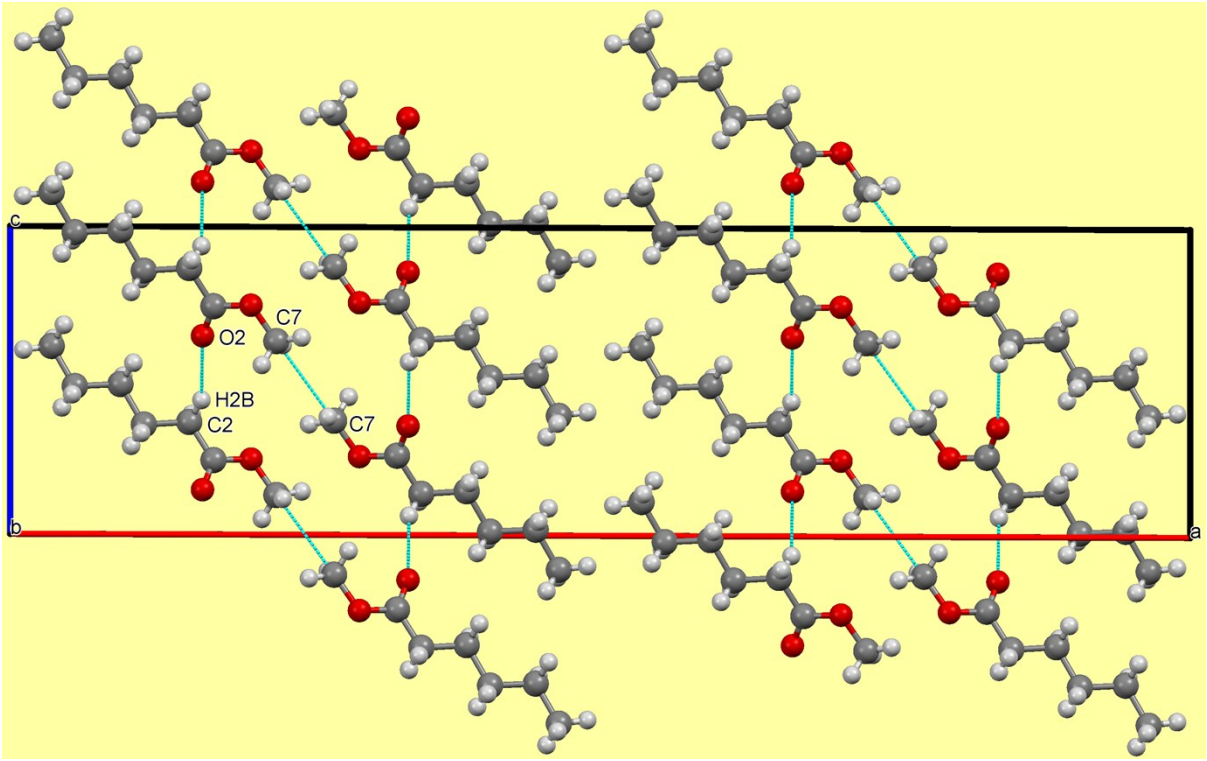

Figure S6. Crystal packing diagram of C_6 methyl ester viewed along the *b*-axis, showing the C(2)-H(2B)···O(2) hydrogen bond and C(7)···C(7) short contact.

B.3 *ORTEP* and Packing Diagrams for C_7 Methyl Ester:

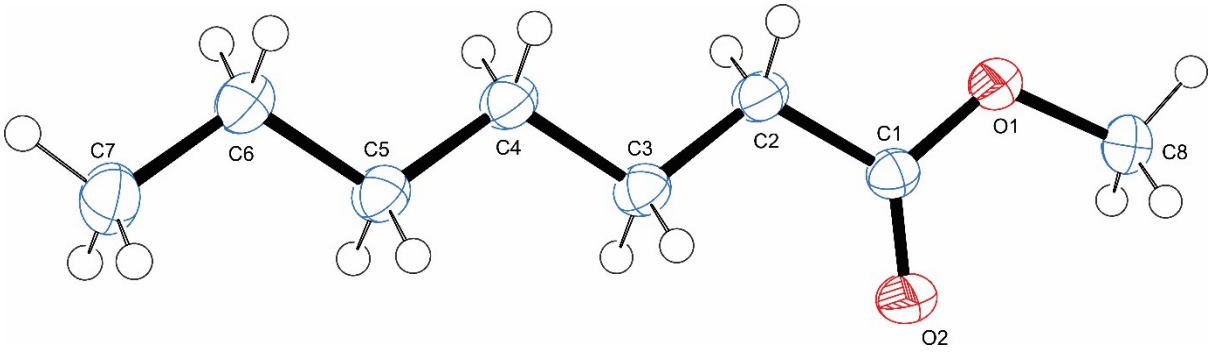

Figure S7. The *ORTEP* diagram of C_7 methyl ester with displacement ellipsoids drawn at the 50% probability level and H atoms are shown as small spheres of arbritary radii.

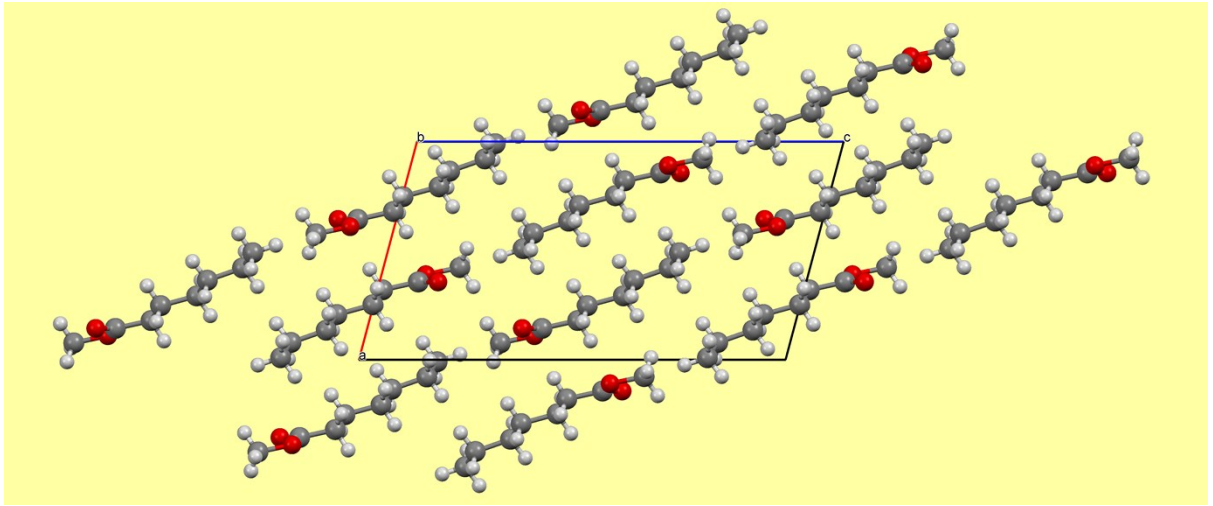

Figure S8. Packing diagram of C_7 methyl ester down the *c*-axis, showing the head-to-tail arangement.

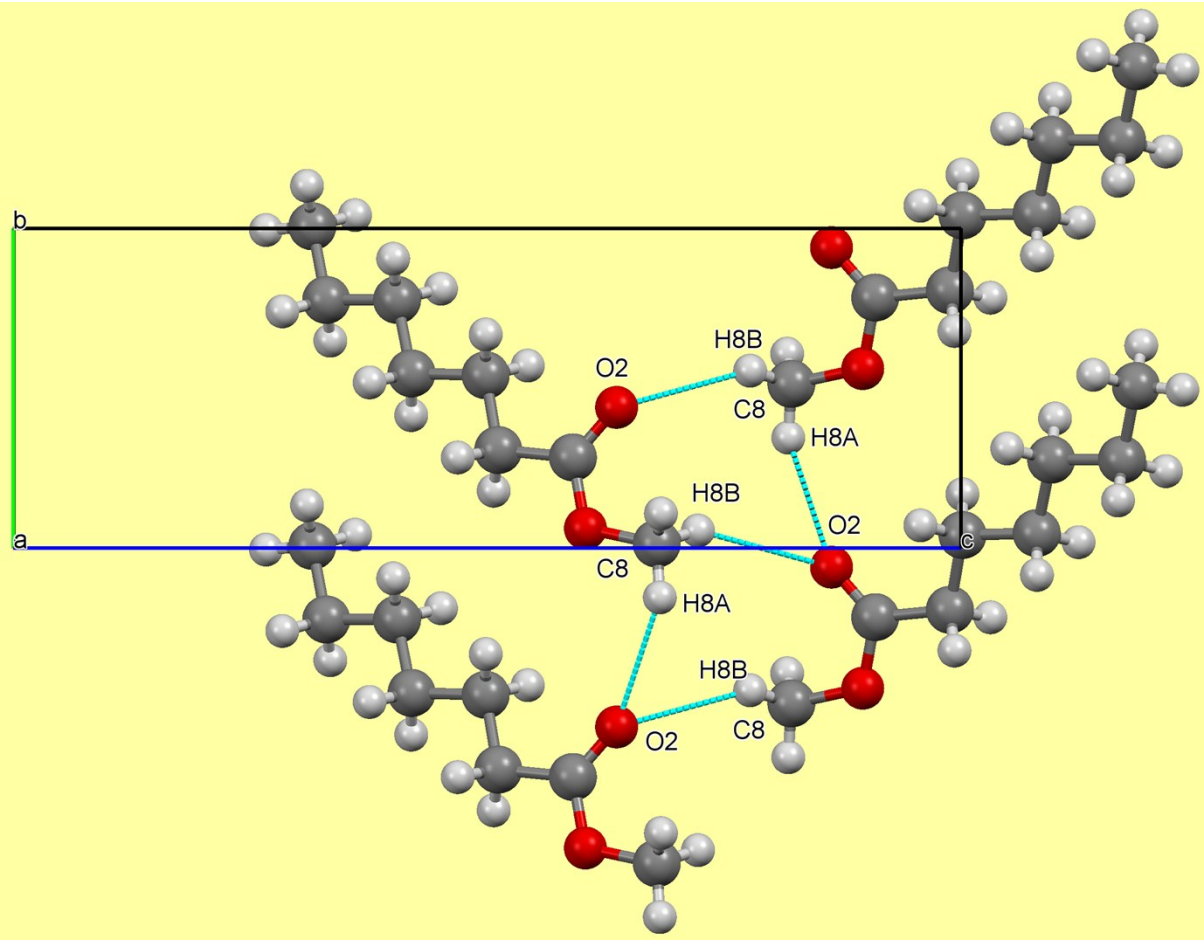

Figure S9. Hydrogen bonding diagram of C_7 methyl ester, showing the C8-H8A···O2 and C8-H8B···O2 hydrogen bonds.

B.4 *ORTEP* and Packing Diagrams for C_8 Methyl Ester:

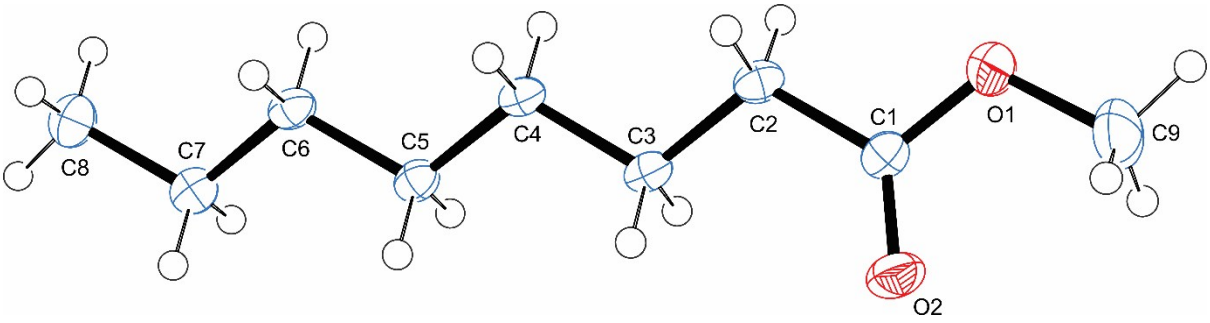

Figure S10. The *ORTEP* diagram of C_8 methyl ester with displacement ellipsoids drawn at the 50% probability level and H atoms are shown as small spheres of arbritary radii.

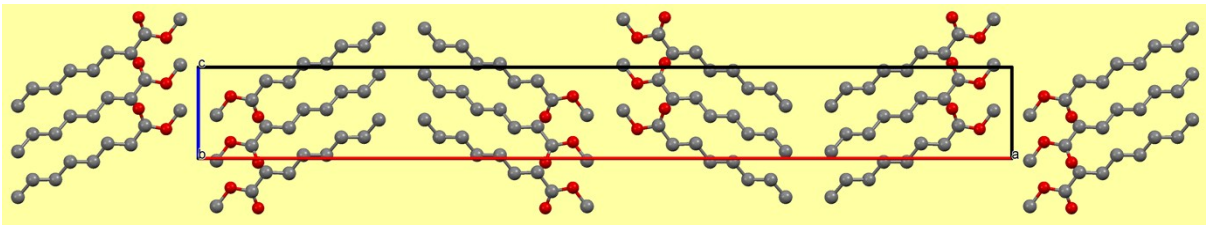

Figure S11. Crystal packing diagram of C_8 methyl ester viewed down *b*-axis, showing the herringbone packing arrangement and the head-to-head arrangement. H atoms omitted for clarity.

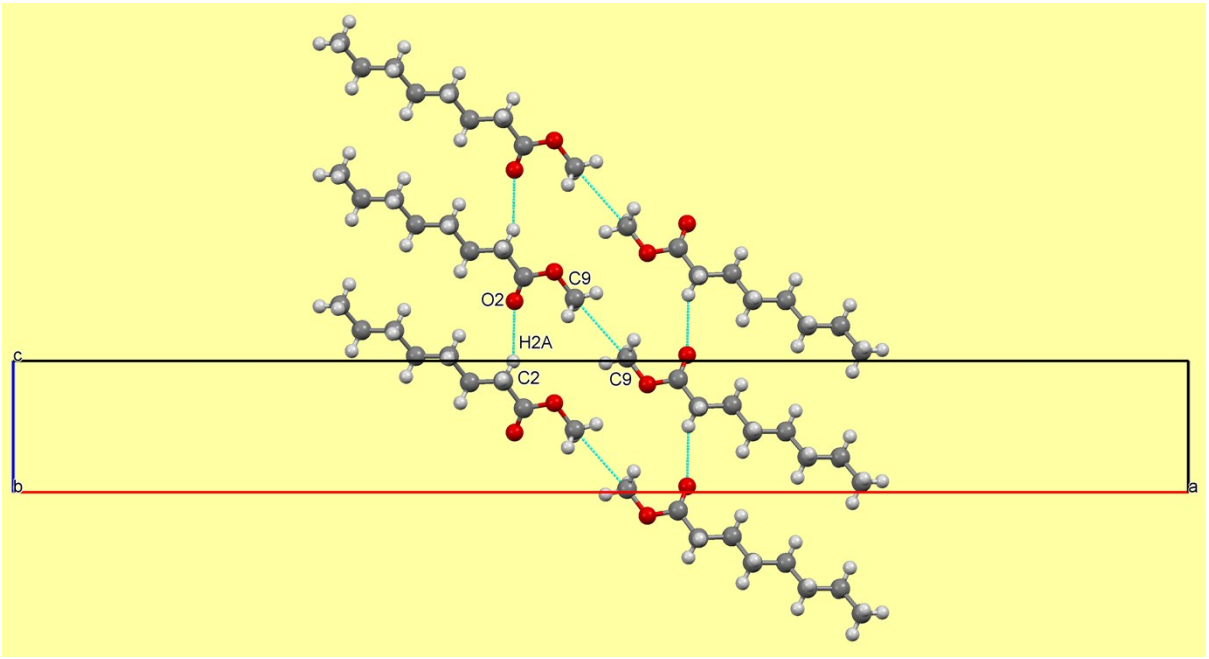

Figure S12. Hydrogen bonding and short contact packing diagram of C_8 methyl ester, showing the C2-H2A···O2 hydrogen bond and C9···C9 short contact.

B.5 *ORTEP* and Packing Diagrams for C_9 Methyl Ester:

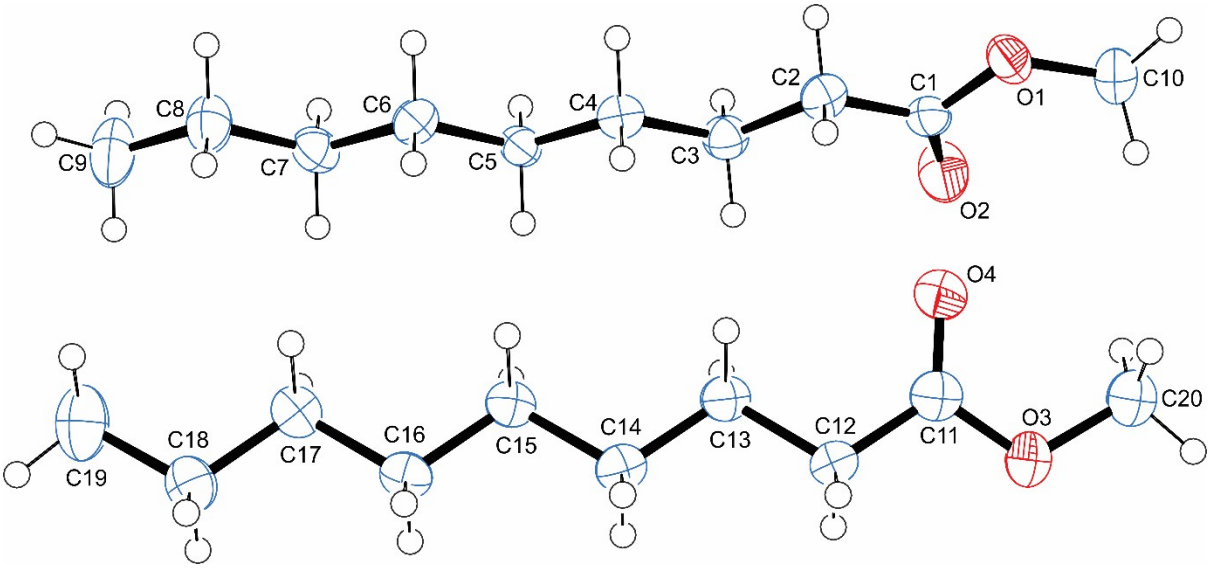

Figure S13. The *ORTEP* diagram of C_9 methyl ester with displacement ellipsoids drawn at the 50% probability level and H atoms are shown as small spheres of arbritary radii.

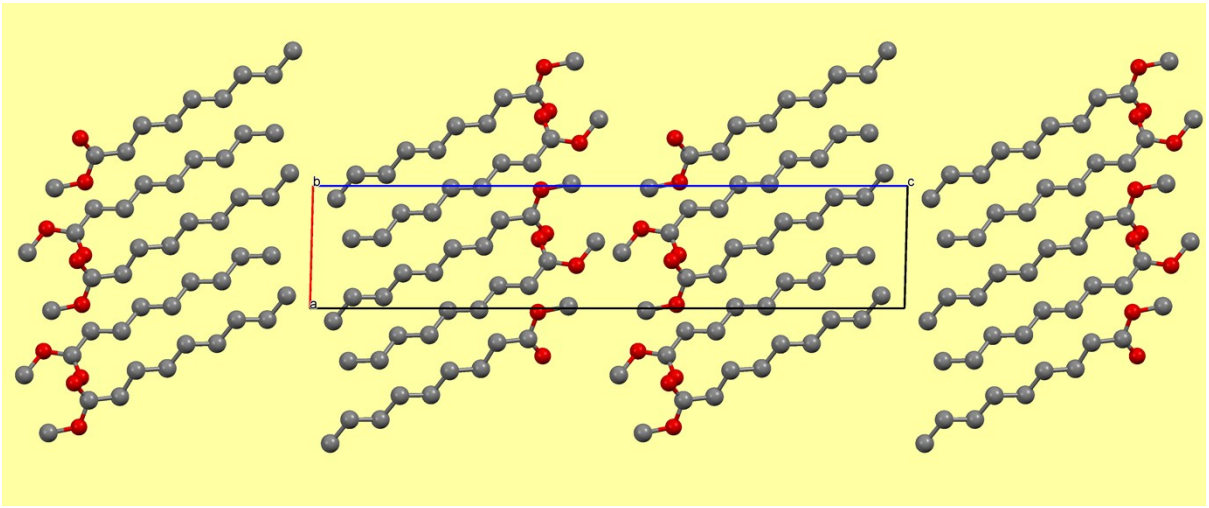

Figure S14. Crystal packing diagram of C_9 methyl ester viewed down *b*-axis, showing the head-to-head parallel stacking.

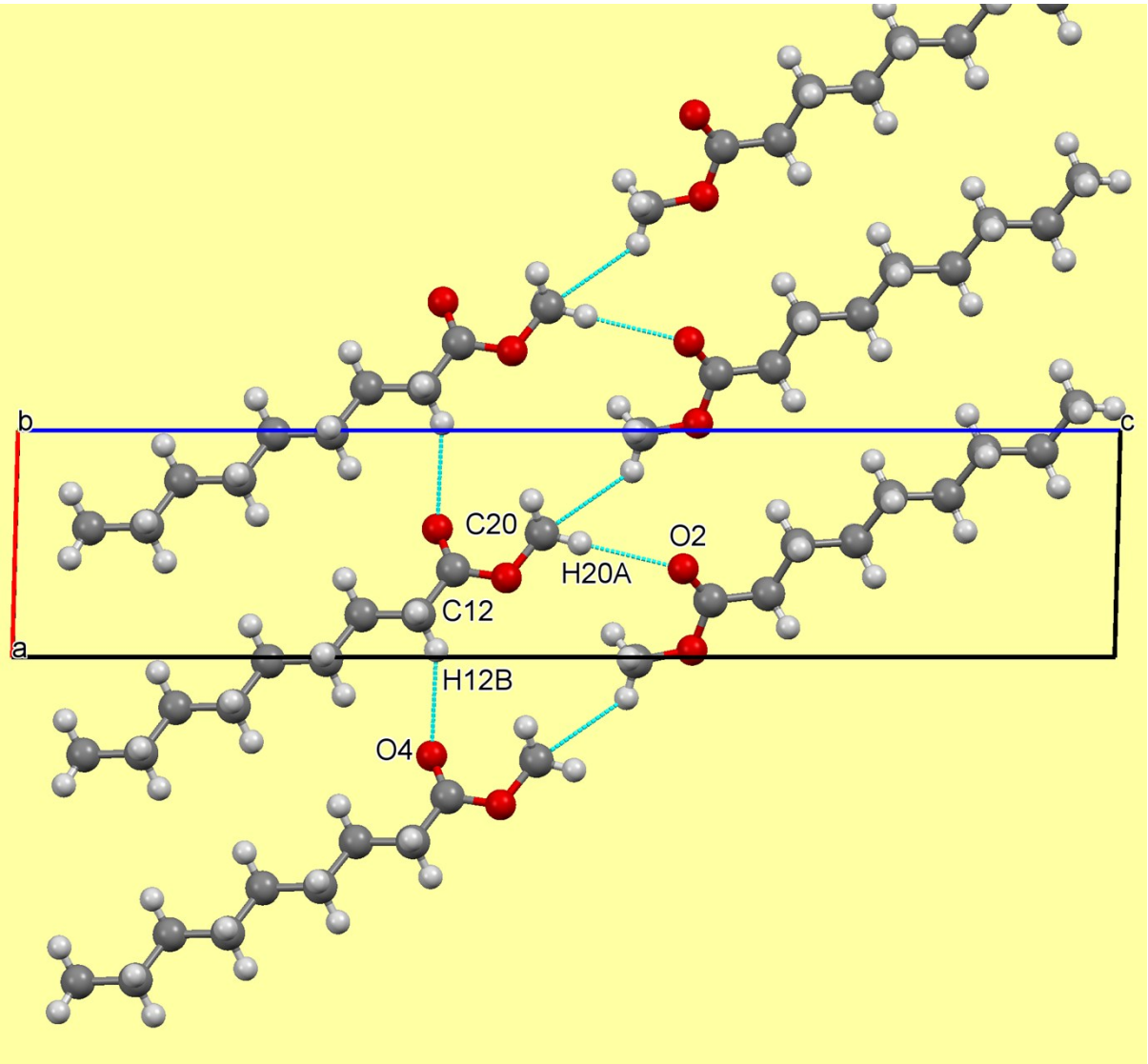

Figure S15. Hydrogen bonding and short contact packing diagram of C_9 methyl ester, showing the C12-H12B···O4 and C20-H20A···O2 hydrogen bond.

B.6 *ORTEP* and Packing Diagrams for C_{10} Methyl Ester:

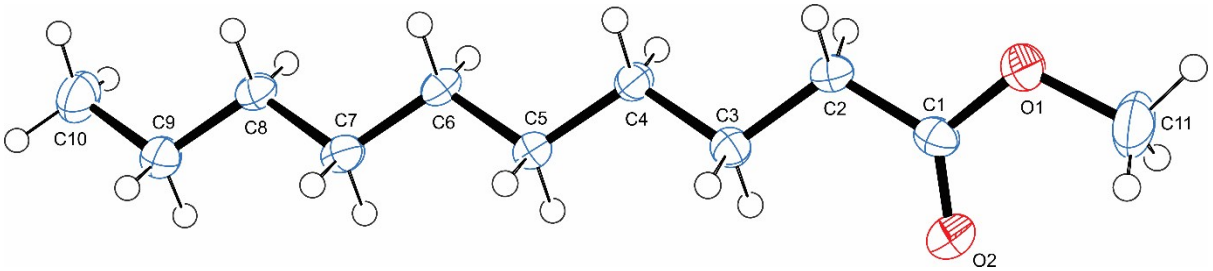

Figure S16. The *ORTEP* diagram of C_{10} methyl ester with displacement ellipsoids drawn at the 50% probability level and H atoms are shown as small spheres of arbritary radii.

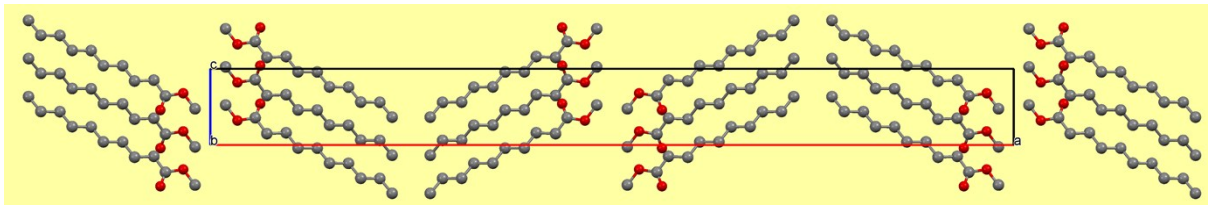

Figure S17. Crystal packing diagram of C_{10} methyl ester viewed down *b*-axis, showing the herringbone packing arrangement and the head-to-head arrangement. H atoms omitted for clarity.

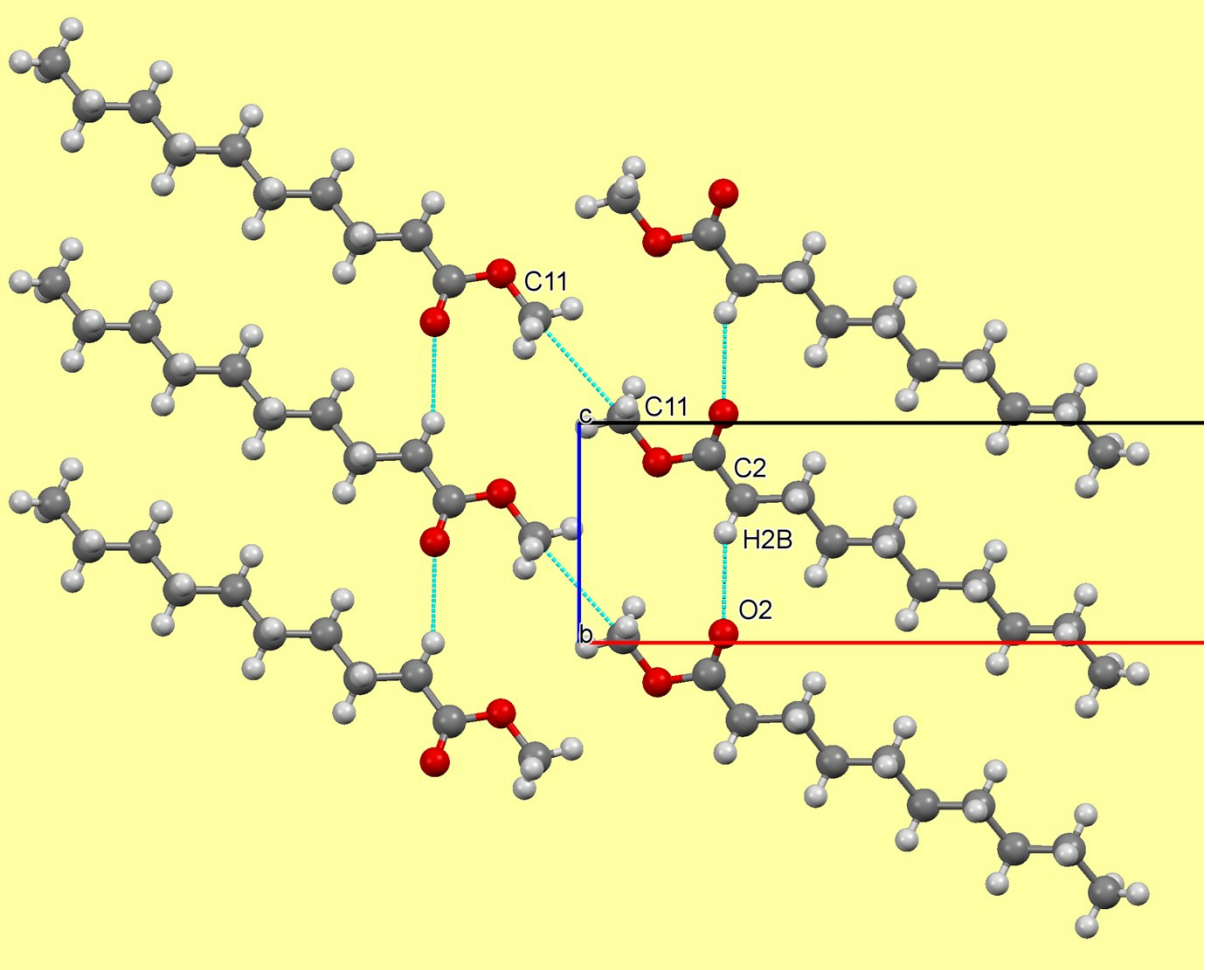

Figure S18. Hydrogen bonding and short contact packing diagram of C_{10} methyl ester, showing the C2-H2B···O2 hydrogen bond and C11···C11 short contact.

B.7 *ORTEP* and Packing Diagrams for C_{11} Methyl Ester:

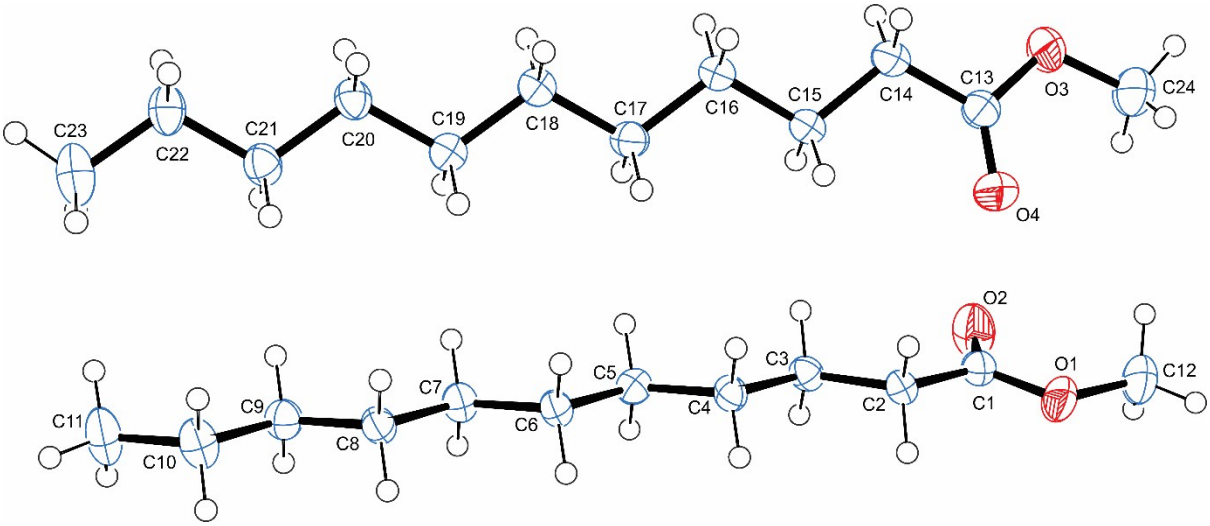

Figure S19. The *ORTEP* diagram of C_{11} methyl ester with displacement ellipsoids drawn at the 50% probability level and H atoms are shown as small spheres of arbritary radii.

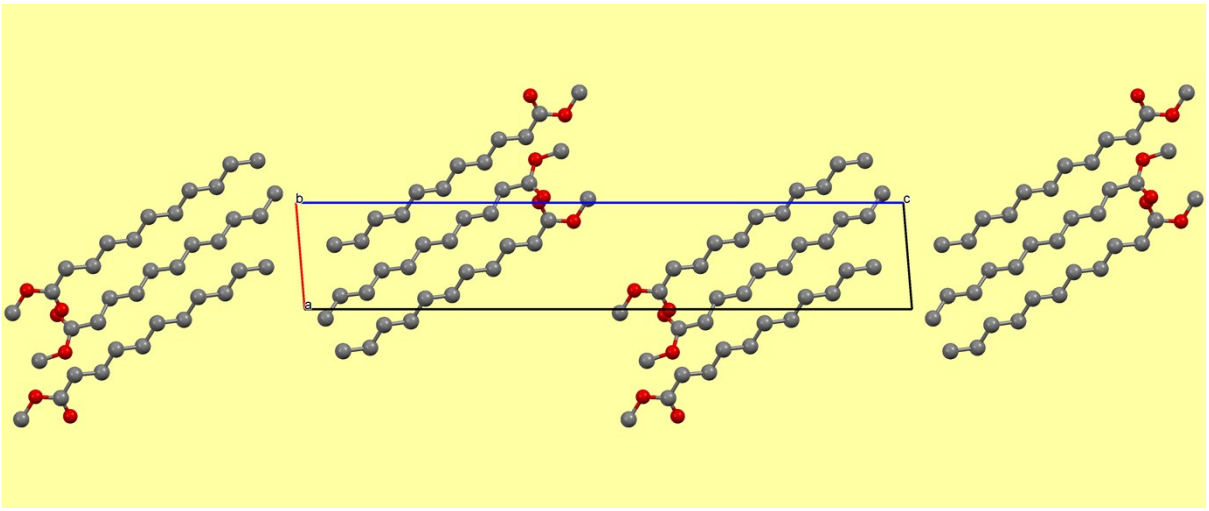

Figure S20. Crystal packing diagram of C_{11} methyl ester viewed down *b*-axis, showing the head-to-head parallel stacking.

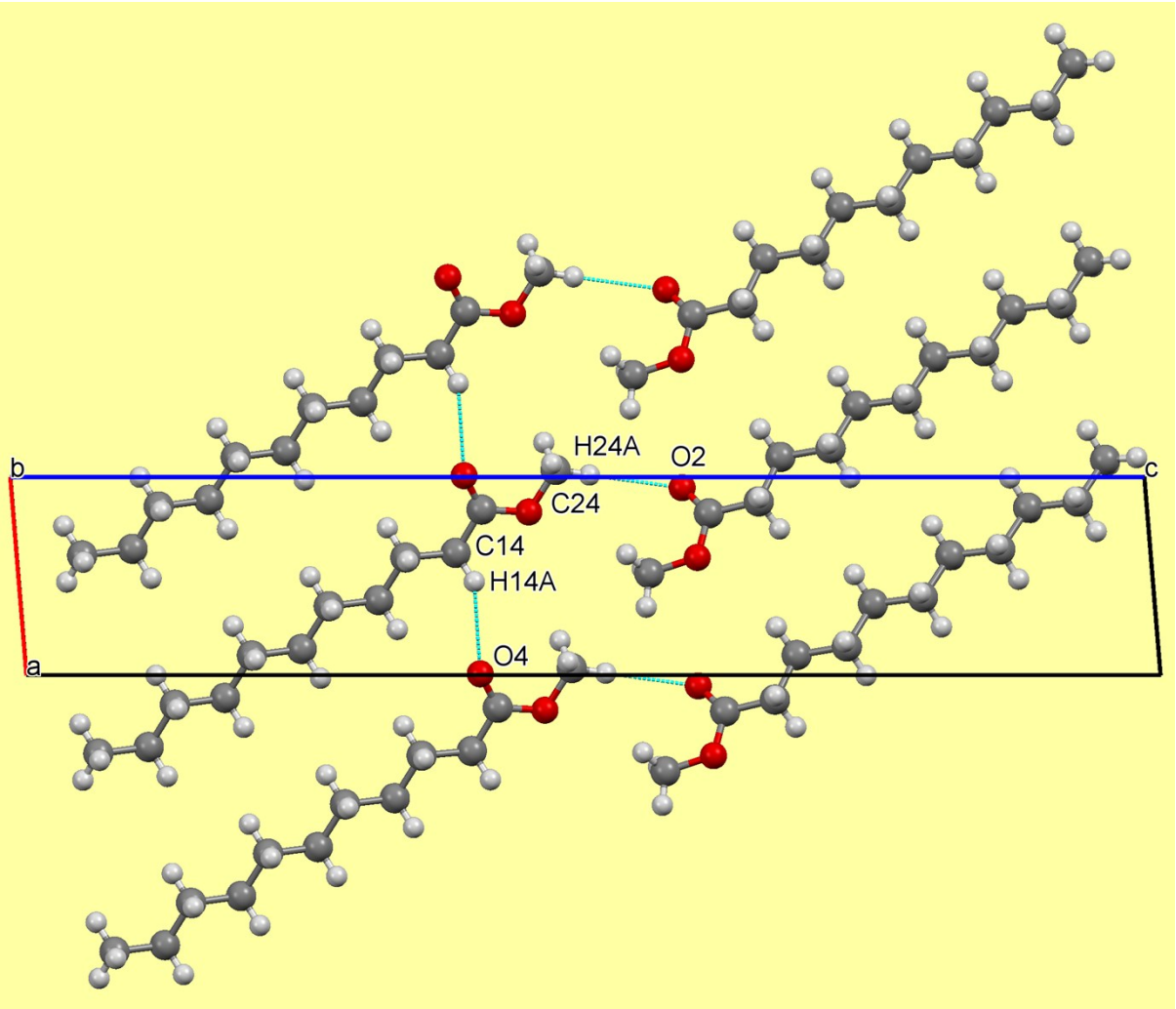

Figure S21. Hydrogen bonding and short contact packing diagram of C_{11} methyl ester, showing the C14-H14A···O4 and C24-H24A···O2 hydrogen bond.

B.8 *ORTEP* and Packing Diagrams for C_{12} Methyl Ester:

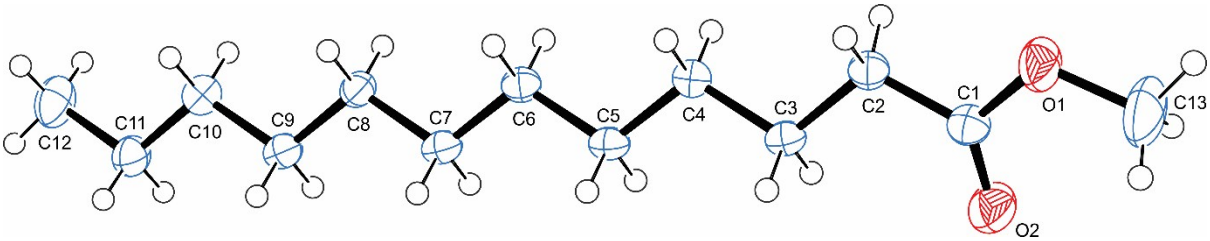

Figure S22. The *ORTEP* diagram of C_{12} methyl ester with displacement ellipsoids drawn at the 50% probability level and H atoms are shown as small spheres of arbritary radii.

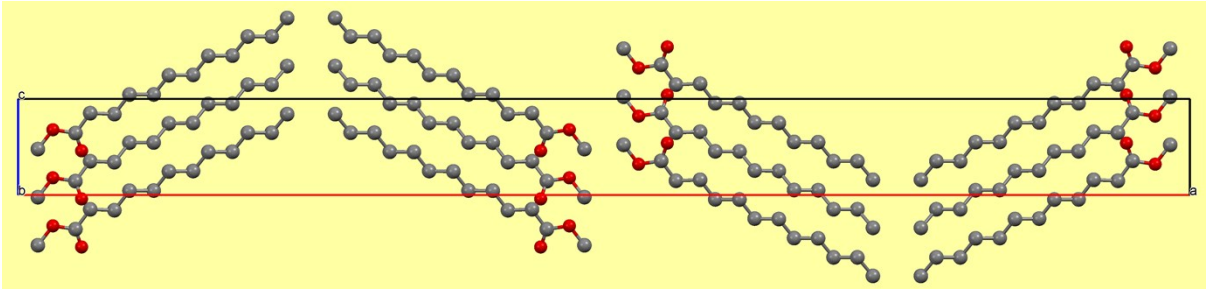

Figure S23. Crystal packing diagram of C_{12} methyl ester viewed down *b*-axis, showing the herringbone packing arrangement and the head-to-head arrangement. H atoms omitted for clarity.

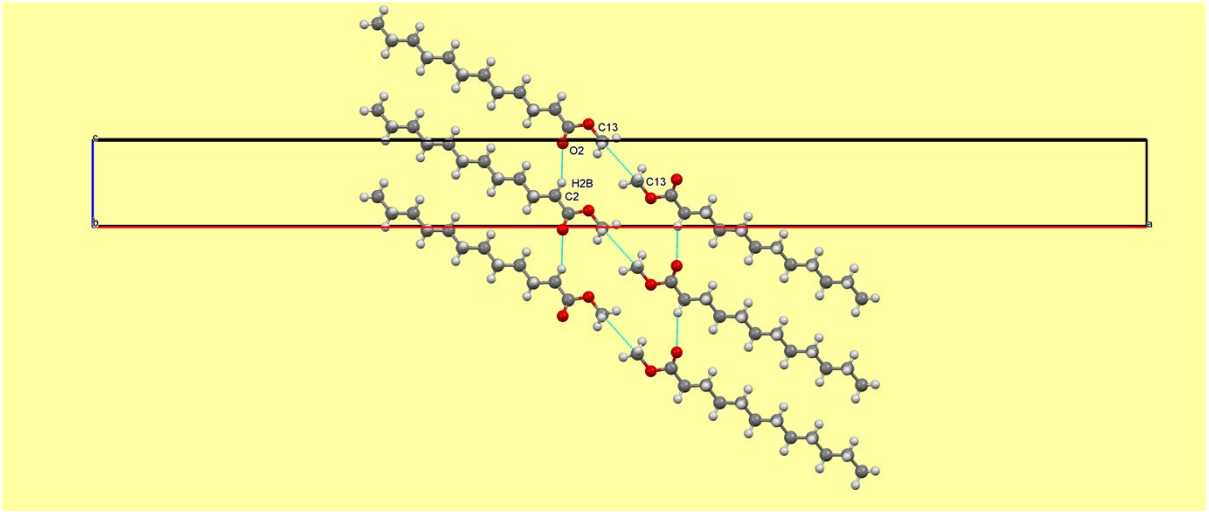

Figure S24. Hydrogen bonding diagram of C_{12} methyl ester, showing the C2-H2B···O2 hydrogen bond.

B.9 *ORTEP* and Packing Diagrams for C_{13} Methyl Ester:

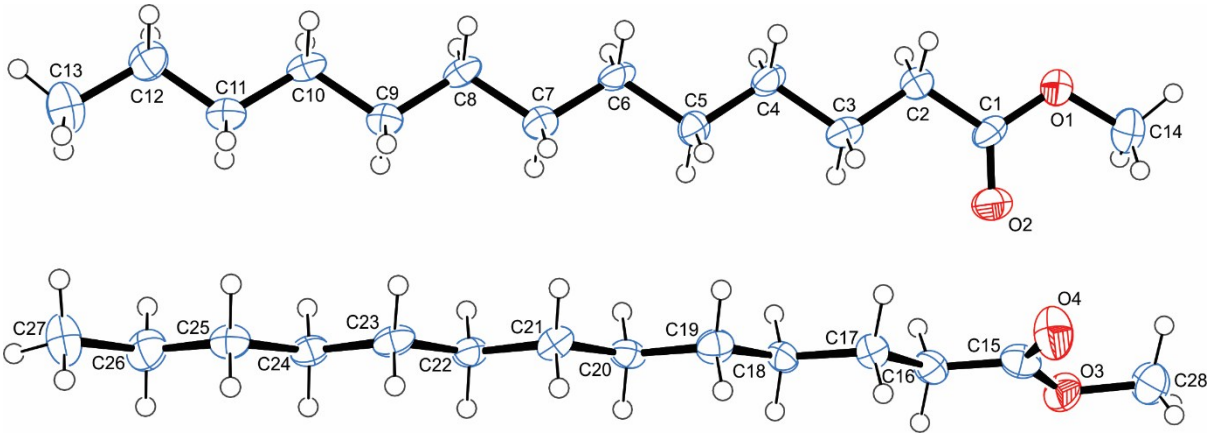

Figure S25. The *ORTEP* diagram of C_{13} methyl ester with displacement ellipsoids drawn at the 50% probability level and H atoms are shown as small spheres of arbritary radii.

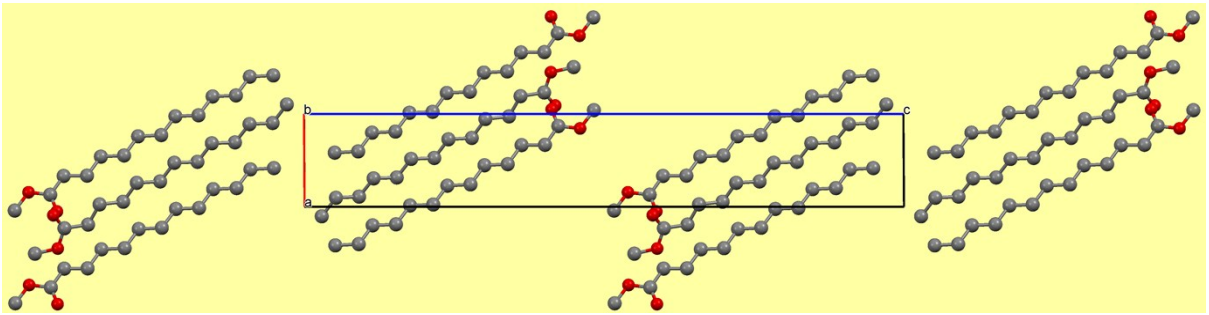

Figure S26. Crystal packing diagram of C_{13} methyl ester viewed down *b*-axis, showing the head-to-head parallel stacking.

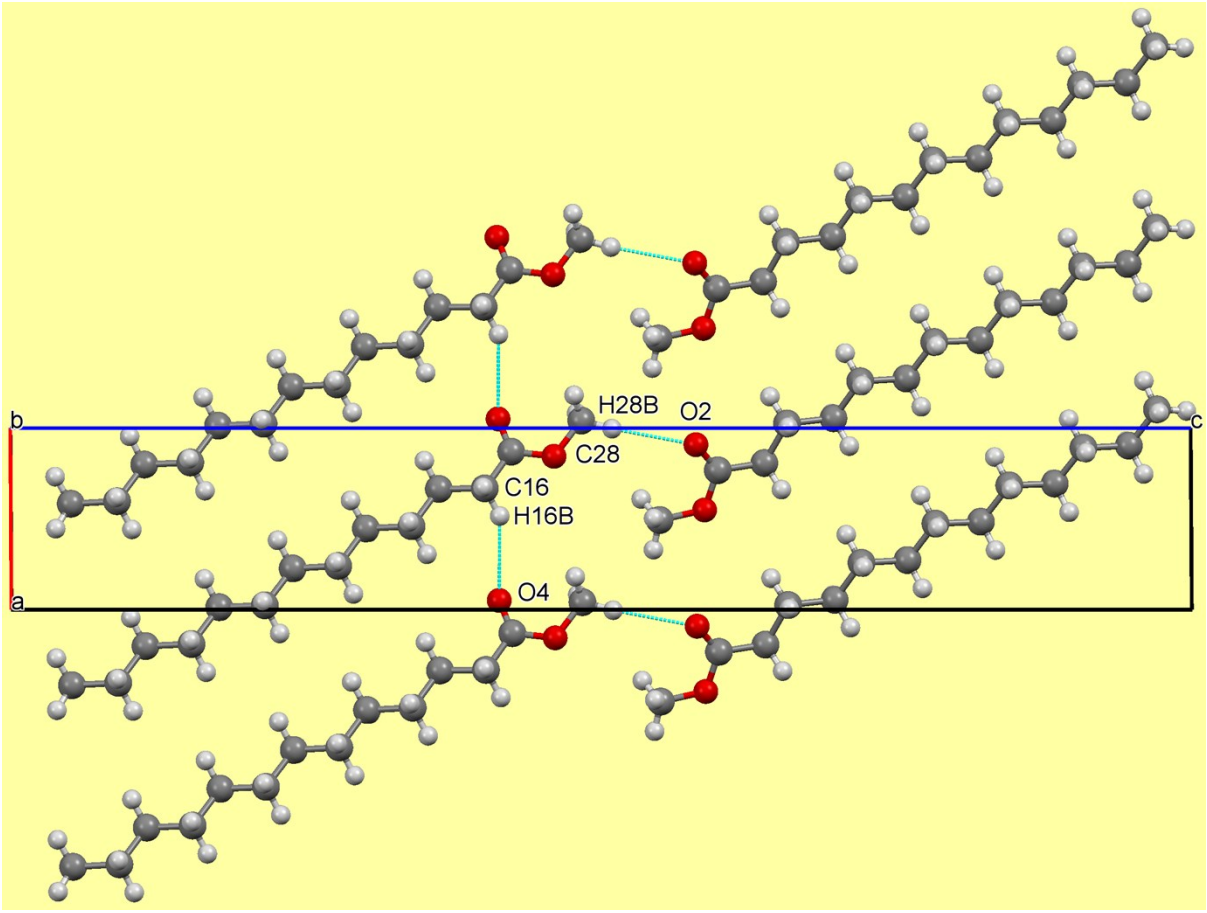

Figure S27. Hydrogen bonding and short contact packing diagram of C_{13} methyl ester, showing the C16-H16B···O4 and C28-H28B···O2 hydrogen bond.

C. DSC Scans for FAME

Table S2 Literature and experimental melting point determined by DSC

Methyl ester	CAS	Melting Point Lliterature[1] / °C	Melting Point (DSC) / °C
C_5	624-24-8	-90.65	-
C_6	106-70-7	-69.55	-
C_7	106-73-0	-55.75	-
C_8	111-11-5	-36.65	-38.3
C_9	1731-84-6	-34.35	-38.9
C_{10}	111-42-9	-12.75	-14.8
C_{11}	1731-86-8	-11.35	-14.2
C_{12}	111-82-0	4.85	+4.1
C_{13}	1731-88-0	5.85	+3.1

1 N. Adriaanse, H. Dekker and J. Coops, *Recl. Trav. Chim. Pays-Bas*, 1964, **83**, 557.

C.1 C_8 Methyl Ester

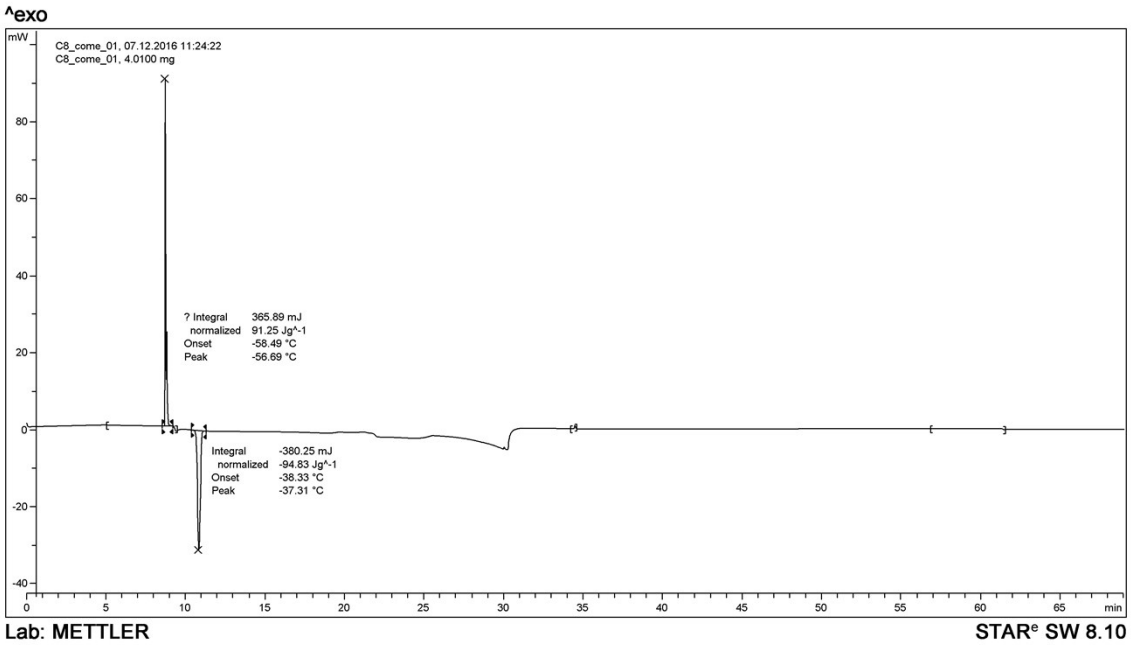

C.2 C_9 Methyl Ester

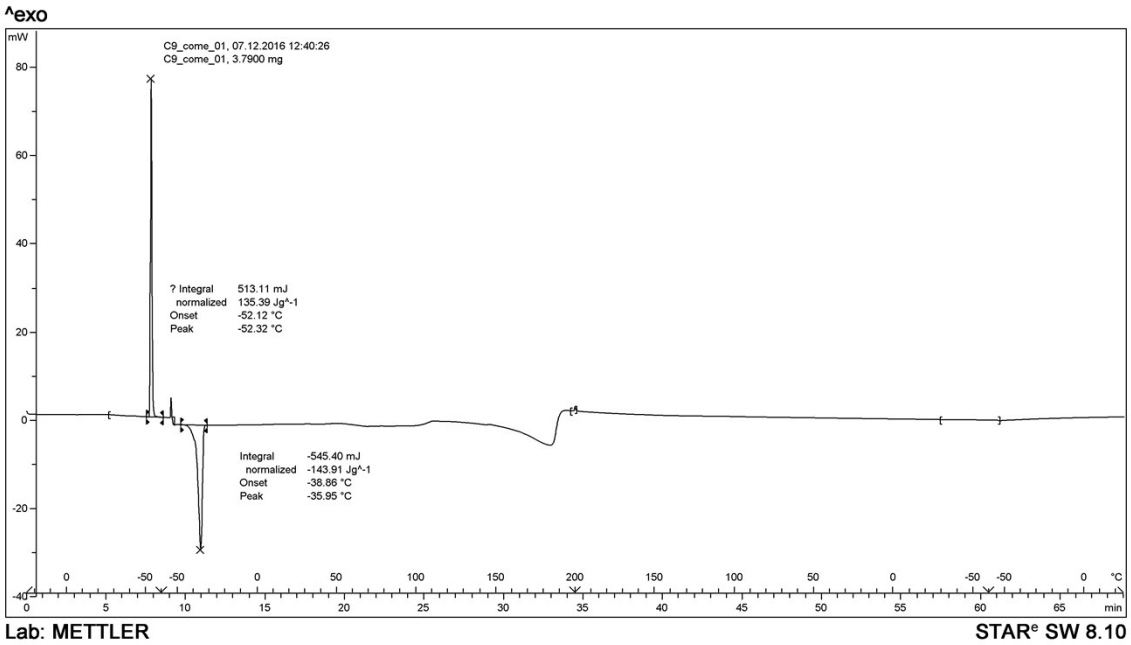

C.3 C_{10} Methyl Ester

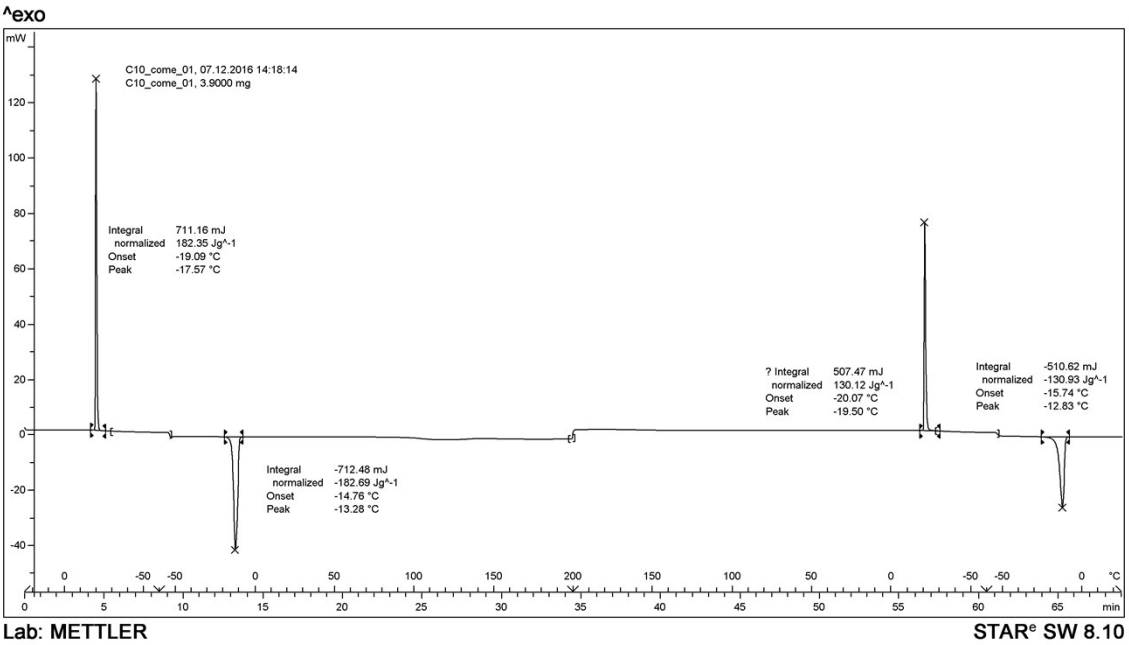

C.4 C_{11} Methyl Ester

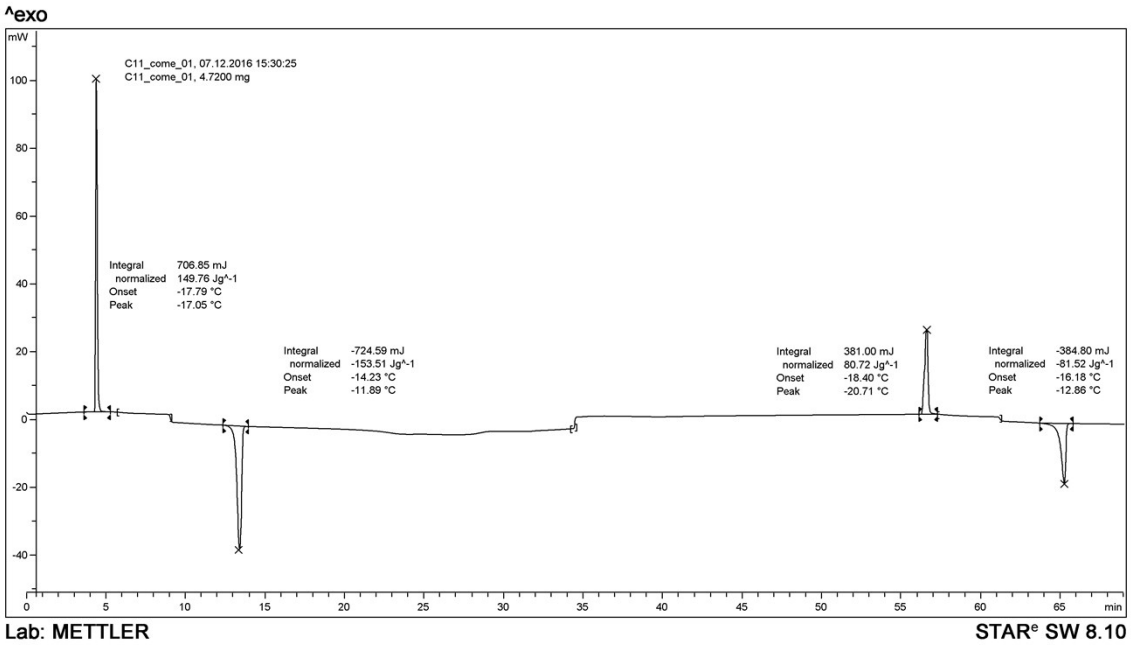

C.5 C_{12} Methyl Ester

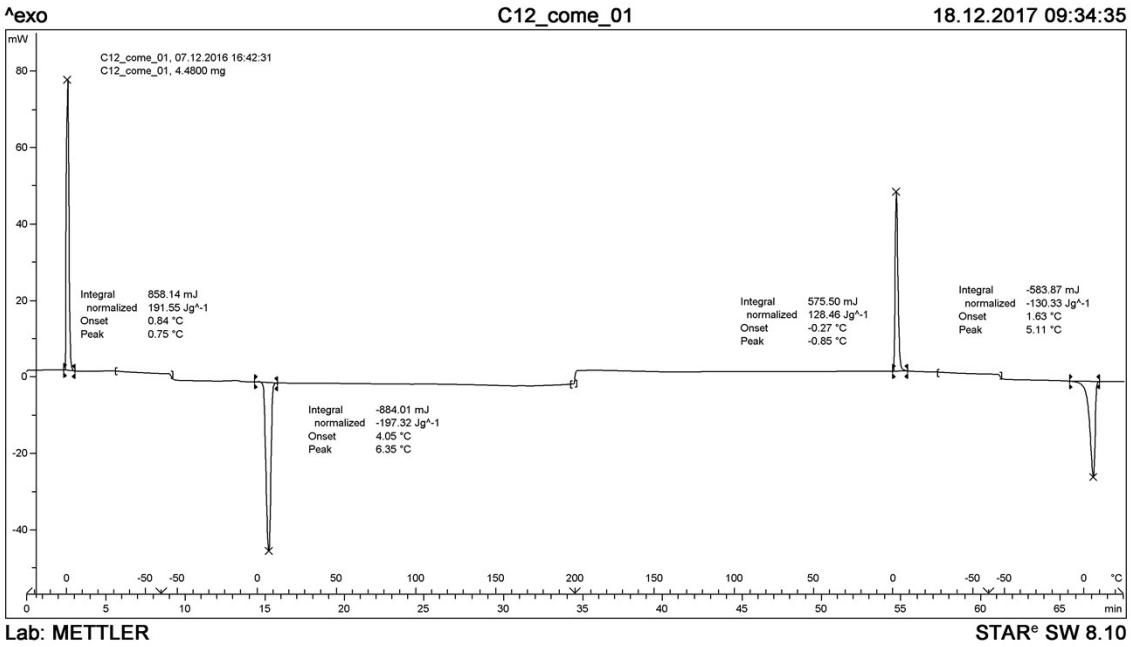

C.6 C_{13} Methyl Ester

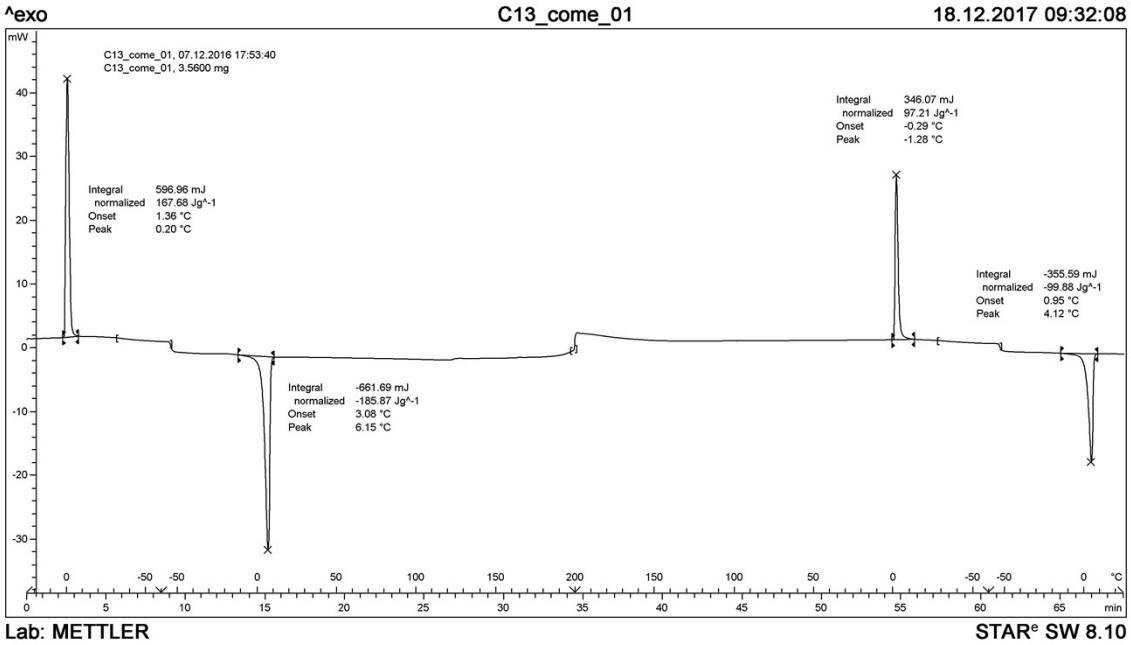

D.1 Hirshfeld surfaces analysis – Fingerprint plots

Figure S20. Fingerprint plots for the C_5 to C_7 FAMEs, resolved into O···H (left) and H···H contacts (right), with the full fingerprint plot as a grey shadow beneath each decomposed plot.

Figure S21. Fingerprint plots for the even- (left) and odd-numbered members (right) of the C_8 to C_{13} FAMEs, resolved into O···H (left) and H···H contacts (right), with the full fingerprint plot as a grey shadow beneath each decomposed plot.